JOURNAL OF VIROLOGY, Jan. 1995, p. 365–375 Vol. 69, No. 1
0022-538X/95/$04.00+0

Human Immunodeficiency Virus Type 1 MA Deletion Mutants Expressed in Baculovirus-Infected Cells: *cis* and *trans* Effects on the Gag Precursor Assembly Pathway

NATHALIE CHAZAL, BERNARD GAY, CHRISTIAN CARRIÈRE, JEANNETTE TOURNIER, AND PIERRE BOULANGER*

Laboratoire de Virologie et Pathogénèse Moléculaires, CNRS URA-1487, Faculté de Médecine, Institut de Biologie, 34060 Montpellier, France

Received 28 July 1994/Accepted 14 October 1994

The role of the matrix protein (MA) of human immunodeficiency virus type 1 in intracellular transport, assembly, and extracellular release of Gag polyprotein precursor (Pr55^{gag}) was investigated by deletion mutagenesis of the MA domain of recombinant Gag precursor expressed in baculovirus-infected cells. In addition, three carboxy-terminally truncated forms of the Gag precursor, representing mainly the MA, were constructed. One corresponded to an MA with a deletion of its last 12 residues (*amb*120), while the others corresponded to the entire MA with an additional sequence from the N-terminal portion of the CA (*amb*143 and *och*180). Deletions within the MA central region (residues 41 to 78) appeared to be detrimental to Gag particle assembly and budding from the plasma membrane. A slightly narrower domain, between amino acids 41 and 68, was found to be critical for soluble Gag secretion. Mutations which totally or partially deleted one or the other of the two polybasic signals altered the transport of N-myristylated Gag precursor to the plasma membrane. In coexpression with wild-type Gag precursor, a discrete *trans*-dominant negative effect on wild-type Gag particle assembly and release was observed with deletion mutants located in the central MA region (residues 41 to 78). A more significant negative effect was obtained with the two recombinant proteins of *amb*120 and *och*180, which redirected the Gag particle assembly pathway from the plasma membrane compartment to intracellular vesicles (*amb*120) and to the nuclear compartment (*och*180).

Multiple structural and physiological functions have been assigned to the matrix proteins (MA) of retroviruses in general and that of human immunodeficiency virus type 1 (HIV-1) in particular (reviewed in reference 46). At late stages of the virus cycle, the MA is a key factor in virion morphogenesis, via its role in (i) intracellular transport (10, 50), (ii) plasma membrane targeting of Gag precursor (Pr55^{gag}) and extracellular budding of membrane-enveloped virions (4, 13, 14, 17, 28, 30, 31, 34, 38, 39, 47, 51), and (iii) virion incorporation of viral glycoproteins (9, 45, 48, 49). At early steps of the virus cycle, the MA may be involved in penetration of cells by the virions and in virus infectivity (8, 44, 49). Additional MA properties, such as (i) coencapsidation of unmyristylated Gag-Pol polyproteins (29), (ii) association with the viral genome and transport of viral preintegration complex to the nucleus (5, 6), and (iii) influence on the binding of Pr55^{gag} to viral RNA in vitro (7), have been reported.

The signals responsible for some of these MA functions have been identified, whereas others are still hypothetical. Targeting to the plasma membrane, virus assembly, and budding depend directly or indirectly upon the myristylation at the N terminus of the MA domain of the Gag precursor (28, 30–32, 34, 38), whereas nuclear addressing and binding to genomic RNA can be mediated by one or two potential karyophilic signals located at residues 26 to 32 (KKKYKLK) and 110 to 114 (KSKKK) in the HIV-1 MA. Likewise, the reported role of the MA domain in HIV-1 infectivity has been hypothesized to be associated with a specific sequence (AADTGHSSQV) at residues 119 to 128 in the MA carboxy terminus, which has strong homology with structural proteins of most picornaviruses and flaviviruses (2, 49). However, membrane binding of Gag precursor and virus particle formation and stability are likely results of the combination of discrete intermolecular interactions, in which multiple peptide sequences and the overall conformation of structural proteins can participate (9, 26, 32, 33, 39, 51).

In cells infected with recombinant baculovirus expressing N-myristylated Gag precursor, Gag particles are efficiently assembled and released by budding from the plasma membrane, even in the case of Gag precursors lacking the NC domain (Pr42^{gag}), provided that the p2 junction peptide at the CA-NC junction (19, 25) is not deleted (15, 21, 36). On the other hand, unmyristylated Gag precursors are also released at high levels into Sf9 cell culture medium, albeit in soluble form, implying that secretion of unassembled Gag polyprotein molecules is not dependent upon myristyl modification of the N terminus, but upon the presence and accessibility of another signal(s). The highest efficiency in secretion of soluble Gag has been observed with nucleocapsid-deleted Pr41^{gag}, suggesting that the signal recognized by a putative membrane receptor is located within amino acids 15 to 375 in the Gag sequence (36). The observation that the Pr39^{gag} cleavage product accumulated by the insertion mutant *in*40, which consisted of the p24^{CA} and p15^{NC} domains, was not found in detectable amounts in the culture medium (7) strongly suggested that the secretion signal for soluble Gag polyprotein is localized in the MA.

In order to further dissect the mechanisms of intracellular transport and extracellular release of membrane-enveloped Gag particles and soluble Gag polyproteins, we generated a panel of mutants with deletions (*dl*) in the MA domain of HIV-1 Gag precursor and analyzed their resulting phenotypes

* Corresponding author. Mailing address: Laboratoire de Virologie & Pathogénèse Moléculaires, Institut de Biologie, 2, Boulevard Henri IV, 34060 Montpellier Cedex, France. Phone: (33) 67 60 57 38. Fax: (33) 67 54 23 78. Electronic mail address: boulange@arthur.citi2.fr.

TABLE 1. Amino acid sequences of MA internal deletion mutants and carboxy-truncated Gag mutants[a]

Mutant designation	WT sequence[b]	Mutant sequence[b]	Origin[c]
*dl*10-21[d]	10-**G**GELDRWEKIR**L**-21	10-**G**–**L**-21	D1
*dl*20-32	20-**R**LRPGGKKKYKL**K**-32	20-**R**–**K**-32	D2
*dl*31-41	31-**L**KHIVWASRE**L**-41	31-**L**–**I**-41	D3
*dl*41-57	41-**L**ERFAVNPGLLETSEG**C**-57	41-**L**–**C**-57	D4
*dl*56-68	56-**G**CRQILGQLQPS**L**-68	56-**G**–**L**-68	D5
*dl*67-78	67-**S**LQTGSEELRS**L**-78	67-**S**–**I**78	D6
*dl*78-91	78-**L**YNTVATLYCVHQ**R**-91	78-**L**–**R**-91	D7
*dl*90-104	90-**Q**RIEIKDTKEALDK**I**-104	90-**Q**–**I**-104	D8
*dl*104-115	104-**I**EEEQNKSKKK**A**-115	104-**L**–**A**-115	D9
*dl*115-129	115-**A**QQAAADTGHSSQV**S**-129	115-**A**–**S**-129	D10
*dl*42-100	42-**E**[43-99]**A**-100	42-**E**–L–**A**-100	
*amb*120	120-**A**DTGH . . .[e]	120-**A**GILV-stop	
*amb*143	143-**V**HQAISP . . .[e]	143-**V**WNSSLD-stop	
*och*180	180-**T**PQD . . .[e]	180-**T**HKI-stop	

[a] Each one of the fourteen deletion (*dl*) mutants presented in the table was constructed in both N-myristylated and unmyristylated versions.
[b] With the exception of L-to-I substitutions at positions 41 and 78, and the I-to-L substitution at residue 104, the WT Gag amino acids which were unchanged in the mutant sequences are in boldface type, and deleted or foreign residues are in standard characters.
[c] Nomenclature of the proviral clones (48, 49) from which our recombinant baculovirus mutants were derived.
[d] The amino acid numbering started from the initiation methionine of the *gag* gene sequence at nucleotide 336 in the HIV-1_{LAV} sequence (43).
[e] Ellipsis indicates that the sequence continues.

in a baculovirus expression system (7, 20, 35, 36). The effects of these deletions in *cis* were studied by using singly infected cells, and those in *trans* were studied by using coexpression with wild-type (WT) $Pr55^{gag}$. We found that none of the *dl* mutants in their unmyristylated versions assembled intracellular core-like particles. In the N-myristylated $Pr55^{gag}$, the deletions in the MA central region, within residues 41 to 78, were detrimental to assembly and budding of membrane-enveloped Gag particles. The deletion of either one or the other consensus karyophilic signal affected the intracellular localization of the mutant Gag particles. Furthermore, a significant *trans*-dominant negative effect was observed in coinfections of WT $Pr55^{gag}$ with two forms of recombinant MA proteins, *amb*120 and *och*180. Coexpression with *amb*120 resulted in a massive accumulation of membrane-enveloped particles within intracytoplasmic vesicles, whereas *och*180 redirected the Gag particle assembly process towards the nucleus. Electron microscope autoradiography (EM-ARG) provided some evidence that intranuclear molecules of HIV-1 $Pr55^{gag}$ could be N myristylated.

MATERIALS AND METHODS

Nomenclature. Each internal deletion (*dl*) mutant is abbreviated by a block of two numbers corresponding to the two codons which immediately preceded and followed the deletion, starting from the *gag* initiator methionine (43). For example, *dl*20-32 indicates that the arginine residue specified by codon 20 is immediately followed by lysine, which occupies position 32 in the WT MA sequence (Table 1). The N-myristylated form of each Gag mutant is indicated by the suffix myr+ (e.g., *dl*90-104myr+), and its unmyristylated counterpart is indicated by myr−. For reasons of simplification, the carboxy-truncated mutants were named according to the nature of their stop codon (*amb* or *och*) within the MA or CA sequence and according to the number of the last amino acid of the Gag sequence, regardless of the few foreign C-terminal residues originating from the insertion cassette or linker (Table 1). Thus, *amb*120 referred to the mutant with an amber stop codon placed at position 125 in the construct, which left the first 120 amino acids of the MA unchanged (Table 1).

Virus, cells, and infections. Recombinant baculoviruses were obtained by in vivo recombination in *Spodoptera frugiperda* (Sf9) cells between an intermediate baculoviral plasmid vector containing the entire HIV-1 *gag* gene under the control of the polyhedrin promoter (pGmAc-NGag; 7, 35, 36) and *Bsu*36I-digested DNA from the AcNPV-derived BacPAK6 virus (Clonetech Lab., Palo Alto, Calif.). WT and mutant Gag recombinants were produced in Sf9 cells maintained in Grace's medium supplemented with 10% fetal calf serum, and cells were harvested at 12, 24, 36, and 48 h postinfection (p.i.). In complementation experiments, Sf9 cells were simultaneously infected pairwise with two mutants at a multiplicity of infection of 10 PFU/cell each. In *trans*-dominant assays with WT $Pr55^{gag}$, Sf9 cells were coinfected with the recombinant expressing the Gag mutant and with Gag12myr+ or G2A, expressing N-myristylated WT $Pr55^{gag}$ and unmyristylated full-length $Pr55^{gag}$, respectively. For Gag processing assays in vivo, cells were infected with the recombinant expressing the Gag substrate at 20 PFU/cell for 1 h at room temperature, and then the virus inoculum was removed and the cells were further incubated for 1 h with 10 PFU of the HIV-1 protease-expressing recombinant (PR107; 7, 20, 41) per cell.

Construction of recombinant Gag mutants. Before insertion into the baculovirus vector, all the mutagenesis steps were performed in a pBluescript II KS− plasmid containing the coding sequences for two forms of the HIV-1 *gag* gene, one coding for an N-myristylated WT $Pr55^{gag}$ and the other one coding for the N-myristylation-defective mutant G2A (7). Short internal deletions in the MA were generated as follows. The individual MA deletions D1 to D10, contained in separate plasmids provided by XiaoFang Yu (HXB2-derived sequence [48, 49]), were rescued by PCR amplification with the pair of primers A and B, for the N-myristylated version of Gag precursor, or the pair A* and B, for the non-N-myristylated version. Oligonucleotides A (5′-CCATGGGTGCGAGAGCGTCAGTATTAAGCGGGGGA-3′) and A* (5′-CCCCCATGGCTGCGAGAGCGTCAGTATTAAGCGGGGG-3′) were designed with an *Nco*I site (underlined) at the initiator methionine, and oligonucleotide B overlapped the TAA stop codon (underlined) of *gag* (3′-AGCAGTGTTATTTGTATCCCCC-5′). After being blunted, the PCR products were digested with *Pst*I (codon position 210 in the CA domain) and the fragments were inserted into pBluescript II KS− cut by *Hin*cII and *Pst*I for DNA sequencing. Each deletion-containing segment of the *gag* gene was then excised by digestion with *Nco*I and *Pst*I, and these segments were placed into the same sites of a previously constructed insertion mutant of *gag* which contained a unique insertional *Eco*RI site and thus facilitated the screening (*in*143 [7]). The large deletion *dl*42-100 was created by excising the fragment between the unique insertional *Eco*RI site of our mutant *in*40 and the natural *Hin*dIII site at codon 100 in the MA and religating the blunted ends. The carboxy-truncated mutants *amb*120 and *amb*143 were generated by inserting an amber multistop codon *Xba*I linker (double-stranded 5′-CTAGTCTAGACTAG-3′) into the blunted *Eco*RI site created at codons 120 and 143 by our linker-insertion mutagenesis (7). The carboxy-truncated mutant *och*180 (formerly *och*184 [7]) was isolated as a result of a cloning accident. Its *gag* sequence consisted of the entire MA and the first 48 amino acids from the CA domain. The required oligonucleotides were synthesized by Eurogentec (Seraing, Belgium). The sequences of the mutants are depicted in Table 1.

Electrophoretic and immunological analyses. Proteins were electrophoresed in sodium dodecyl sulfate–12.5% polyacrylamide gels (SDS-PAGE gels; acrylamide-to-bisacrylamide ratio of 50:0.8), by using a discontinuous buffer system (23), and electrically transferred to nitrocellulose membranes (Hybond-ECL; Amersham) at 180 mA for 90 min, by using a semidry system (Cambridge Electrophoresis, Ltd., Cambridge, United Kingdom). After blocking in 5% skim milk in Tris-buffered saline (20 mM Tris-HCl, pH 7.5, 150 mM NaCl) containing 0.05% Tween 20 (TBS-T) for 1 h at room temperature, the Gag proteins were detected on blots by successive reactions with anti-Gag primary antibody at a dilution of 1:1,000 in TBS-T for 16 h at room temperature, alkaline phosphatase-labeled anti-immunoglobulin G conjugate (1:1,000; Sigma), and nitroblue tetrazolium–5-bromo-4-chloro-3-indolylphosphate toluidinium cosubstrate-substrate (Boehringer) for color development. The following primary antibodies were used: (i) mouse monoclonal antibody (MAb) Epiclone-5001, directed against Pr55-p24 (Epitope, Beaverton, Oreg.) and mapped between residues 341 and 357

(7); (ii) anti-Pr55-p17 MAb Epiclone-5003; (iii) anti-Pr55-p17 MAb 3H7 (mapped between residues 113 and 122 [27a]); (iv) anti-p6 rat MAb M35/2F8 (42), mapped between residues 463 and 500 (6a); and (iv) homemade anti-Gag polyclonal antibody, raised in a rabbit by injection of a bacterially expressed glutathione-*S*-transferase-fused (18) p23^{gag} protein, consisting of the MA and the N-terminal third of the CA domain until residue Ala-210 (*Pst*I site). We mapped the Epiclone-5003 epitope to the carboxy-terminal extremity of the MA, between residues 120 and 132, since its reactivity in blots was drastically reduced with our Gag mutant *dl*115-129 and totally abolished with the recombinant MA protein of *amb*120 (data not shown).

Immunological assay for extracellular Gag. Gag protein was assayed as membrane-enveloped particles (N-myristylated Gag) or soluble protein (unmyristylated form) in unfractionated samples of culture fluid from recombinant-infected cells harvested at 48 h p.i. After clarification by centrifugation at 10,000 $\times$ *g* for 10 min, 40-μl aliquots of culture medium from 10^6 cells were denatured with 20 μl of SDS sample buffer and analyzed by SDS-PAGE and enhanced chemiluminescence immunoblotting (7). Luminograms (Hyperfilm-ECL; Amersham) were scanned at 610 nm with an automatic scanner (REP-EDC densitometer system; Helena Laboratories, Beaumont, Tex.). To prevent misevaluations of overexposed bands and to stay within the linear range of response of Gag signals, several exposures of the same immunoblot were made, and linearity was verified by using a series of twofold-diluted samples of WT Pr55^{gag} added as internal standards to each immunoblot. The level of extracellular Gag mutant was expressed as the percentage of N-myristylated WT Pr55^{gag} released by Gag12myr+ or the percentage of unmyristylated soluble Gag secreted by G2A in parallel infected cell cultures, to which were attributed the 100% value.

DNA sequence analysis. Clones carrying deletions in the *gag* gene were verified by sequence analysis of the desired DNA fragment reinserted into pBluescript II KS−, by using the dideoxynucleotide chain termination technique (37). The Sequenase kit version 2.0 from U.S. Biochemical Corp. (Cleveland, Ohio) was used for sequencing, according to the supplier's recommendations. The inserts were usually sequenced from both ends, by using the M13 universal forward and reverse primers. However, for large DNA fragments in which no convenient restriction sites were available for subcloning, oligonucleotides hybridizing to sequences upstream and downstream of the mutations were used for priming.

Viral RNA binding. North Western (NW) blotting was performed under the conditions previously described (7, 21, 24). The ^{32}P-labeled probe corresponded to the 5′-terminal portion of HIV-1$_{LAV}$ genomic RNA (43), overlapping the splice donor site and the start of the *gag* gene. It was obtained by in vitro transcription of the *Sac*I-*Xmn*I fragment (nucleotides 675 to 840) cloned in pBluescript II KS−, by using an RNA transcription kit (Stratagene). Nonspecific probe was transcribed from the complementary strand.

EM and EM-ARG. For conventional electron microscopy (EM), Sf9 cells were infected at a multiplicity of infection of 10 PFU/cell and harvested at 40 to 48 h p.i. The cell pellets were fixed with 2.5% glutaraldehyde in 0.1 M phosphate buffer, pH 7.5, postfixed with osmium tetroxide (2% in H_2O), and treated with tannic acid (0.5% in H_2O). After dehydration, the specimens were embedded in Epon (Epon-812; Fulham, Latham, N.Y.). Sections were stained with 2.6% alkaline lead citrate and 0.5% uranyl acetate in 50% ethanol and examined with a Hitachi H7100 electron microscope. For EM-ARG, [9,10 (*n*)-^{3}H]myristic acid in toluene (1.92 TBq/mmol; Amersham) was dried under vacuum, resuspended in dimethyl sulfoxide, and added to baculovirus-infected cells maintained in serum-free culture medium (7.4 MBq/ml) for 24 h at 16 h p.i. The [^{3}H]myristyl-labeled cell samples were fixed with phosphate-buffered 2.5% glutaraldehyde and embedded in Epon as described above. Grids supporting the cell sections were coated with Ilford nuclear research emulsion L4 in gel form and exposed at 4°C in lightproof boxes containing silica gel as a dessicant (11). Grids were taken at 2-week intervals, and the emulsion was developed by gold latensification (3). Sections were stained with 2% uranyl acetate in H_2O and examined with the electron microscope.

RESULTS

Isolation of MA deletion mutants in recombinant baculovirus. Fourteen mutants with deletions (*dl*) in the *gag* gene of HIV-1 were generated. Each mutant was constructed in its N-myristylated and unmyristylated versions (G2A substitution [7]), and the resulting phenotypes of the Gag precursor mutants were analyzed in a baculovirus expression system (20, 35, 36). Ten short in-frame deletions scanned the entire MA domain. Mutants *dl*10-21, *dl*20-32, *dl*31-41, *dl*41-57, *dl*56-68, *dl*67-78, *dl*78-91, *dl*90-104, *dl*104-115, and *dl*115-129 contained deletions of 9 to 15 residues (48, 49). A larger deletion mutant, *dl*42-100, overlapped a block of five short deletions in the MA central region, spanning residues 43 to 99. In addition, three carboxy-truncated forms of Gag precursor representing mainly the MA protein were constructed. (i) *amb*120 expressed the MA with a deletion of its last 12 residues, including the highly conserved viral sequence within amino acids 119 to 128 (AADTGHSSQV [2]); (ii) *amb*143 expressed the entire MA extended by 11 amino acids from the adjacent N terminus of the CA domain; and (iii) *och*180 codes for the MA extended by 48 amino acids from the CA (Table 1) domain.

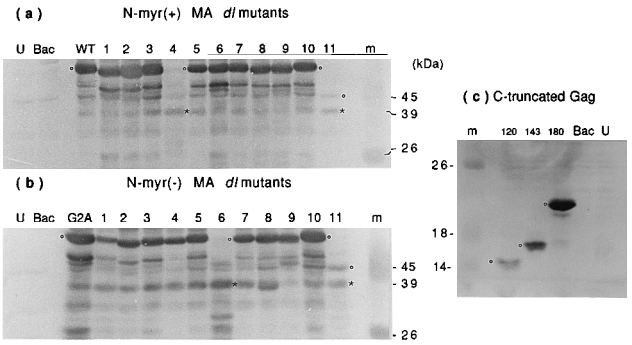

FIG. 1. SDS-PAGE and immunoblot analysis of full-length Pr55^{gag} and Gag deletion mutants expressed in recombinant baculovirus-infected Sf9 cells harvested at 48 h p.i. (a and b) Internal deletion (*dl*) mutants in their N-myristylated (a) and unmyristylated (b) versions. Lanes: 1, *dl*10-21; 2, *dl*20-32; 3, *dl*31-41; 4, *dl*41-57; 5, *dl*56-68; 6, *dl*67-78; 7, *dl*78-91; 8, *dl*90-104; 9, *dl*104-115; 10, *dl*115-129; 11, *dl*42-100; m, prestained molecular mass markers (BRL); U, mock-infected cells; Bac, BacPak6-infected cells; WT, N-myristylated full-length Pr55^{gag} expressed by Gag12myr+; G2A, unmyristylated full-length Pr55^{gag}. (c) Unmyristylated carboxy-truncated Gag mutants. Lanes: 120, *amb*120myr−; 143, *amb*143 myr−; 180, *och*180myr−. Blots a and b were immunoreacted with anti-p24 MAb (Epiclone-5001), and blot c was immunoreacted with two anti-p17 MAbs, Epiclone-5003 and 3H7. Note that *amb*120 lacked the epitope recognized by Epiclone-5003 and only reacted with 3H7. N-Myristylated mutant patterns of *amb*120myr+, *amb*143myr+, and *och*180myr+, similar to the patterns in panel c, are not presented. Primary *gag* gene products are indicated by open dots, and the Pr39^{gag} cleavage product is indicated by asterisks. Numbers to the right of panels a and b and to the left of panel c are molecular masses in kilodaltons.

Synthesis and intracellular processing of MA mutants in Sf9 cells. The level of synthesis, apparent molecular mass, and stability of each Gag mutant were analyzed by SDS-PAGE and immunoblotting of extracts from cells harvested at different times after infection. Most of the mutants showed the expected molecular masses for their recombinant Gag precursors, which accumulated as stable 55- or 54-kDa proteins (Fig. 1). However, for two mutants in each series, *dl*41-57myr+ and *dl*42-100myr+ (Fig. 1a) and *dl*67-78myr− and *dl*42-100myr− (Fig. 1b), only trace amounts of the primary *gag* gene product were visible and a shorter Gag protein species was found at 39 kDa. The possibility of an error in the *gag* sequence was excluded on the basis of mutant DNA sequencing data and time-course synthesis and immunological analysis of the mutant Gag products. The Pr39^{gag} species failed to react with MAb anti-p17 (Epiclone-5003), but it still reacted with rat MAb anti-p6 (data not shown), suggesting that Pr39^{gag} retained the CA and NC domains. This was reminiscent of the *in*40 pattern (7), and it would imply that the MA-CA junction was more accessible to proteolytic cleavage in some mutants than in WT Pr55^{gag}. The recombinant MA proteins expressed by *amb*120, *amb*143, and *och*180 migrated with the expected respective apparent molecular masses of 14.5, 16, and 22 kDa (Fig. 1c).

Processing of Pr55^{gag} at its MA-CA and CA-NC junctions by HIV-1 protease coexpressed in *trans* in Sf9 cells (7, 20) was used as an in vivo qualitative assay for mutant Gag conformational change and domain accessibility. Upon coexpression of recombinant protease, most of the MA internal deletion mutants showed the proteolytic pattern previously described (7), with a major intermediate cleavage product at 39 kDa and two specific discrete bands migrating as a doublet and corre-

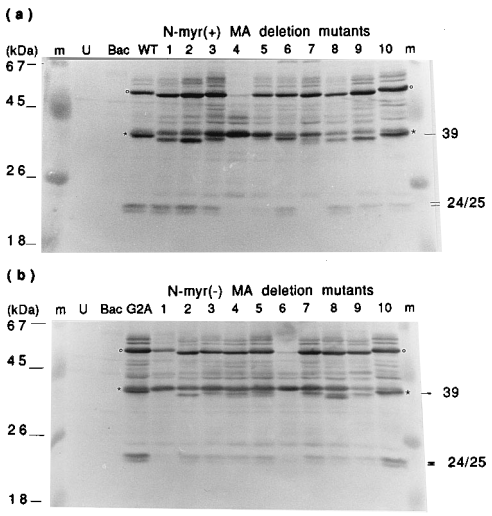

FIG. 2. In vivo processing of MA *dl* mutants by HIV-1 protease coexpressed in *trans* in Sf9 cells. (a) N-Myristylated WT Pr55^{gag} and *dl* mutants. (b) Unmyristylated full-length Gag G2A and *dl* mutants. Cells were harvested at 24 h p.i. and analyzed by SDS-PAGE and immunoblotting with rabbit polyclonal anti-Gag serum. Lanes: m, markers; U, mock-infected cells; Bac, BacPak6-infected cell extracts; 1, *dl*10-21; 2, *dl*20-32; 3, *dl*31-41; 4, *dl*41-57; 5, *dl*56-68; 6, *dl*67-78; 7, *dl*78-91; 8, *dl*90-104; 9, *dl*104-115; 10, *dl*115-129. Numbers at the left are molecular masses in kilodaltons; 39 and 24/25 at the right refer to major Pr55^{gag} cleavage products.

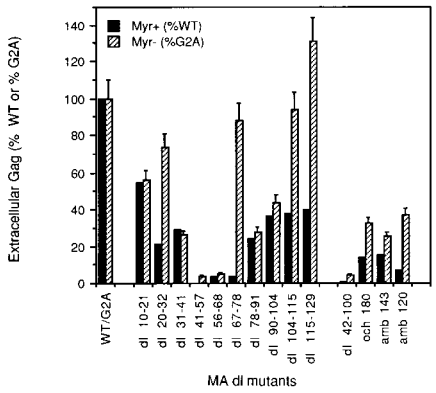

FIG. 4. Extracellular release of Gag by MA *dl* mutants and carboxy-truncated mutants in their N-myristylated (solid columns) or unmyristylated (hatched columns) configuration. The Gag concentration in the growth medium (*y* axis) was expressed as the percentage of the control value, i.e., as the percentage of WT Pr55^{gag} released by Gag12myr+ for the N-myristylated set or as the percentage of soluble Gag protein secreted by G2A for the unmyristylated set. The standard error was 10 to 15% of the reported values ($n = 3$). The internal deletions are positioned along the linear sequence of the MA domain, represented by the *x* axis, from the N terminus to the C terminus. Mutants *dl*42-100, *och*180, *amb*143, and *amb*120 are arbitrarily grouped at the right in the panel.

sponding to the p24-p25CA proteins (Fig. 2). However, three mutants in the N-myristylated series, *dl*41-57myr+, *dl*56-68myr+, and *dl*78-91myr+ (Fig. 2a), and two in the unmyristylated series, *dl*10-21myr− and *dl*67-78myr− (Fig. 2b), showed a lower level of p25-p24 species than did WT Pr55^{gag}. For these mutants, the processing was apparently blocked at the higher-molecular-mass intermediate product Pr39^{gag}, corresponding to the CA-NC domains. Two of these mutants (*dl*41-57myr+ and *dl*67-78myr−) were found to produce unstable Gag precursor, accumulating as a Pr39^{gag} breakdown product in singly infected cells (Fig. 1). For the other mutants, *dl*56-68myr+, *dl*78-91myr+, and *dl*10-21myr−, the lower efficiency in Pr55^{gag} processing suggested a mutation-induced change in their three-dimensional structures which reduced the accessibility of cleavage sites to the protease.

Viral RNA binding in vitro. The capacity of the MA *dl* mutants to bind to a viral RNA probe containing the encapsidation signal (psi) was investigated by NW blotting assays (7, 21, 24). As shown in Fig. 3, no binding was detectable for the large deletion mutant *dl*42-100myr+ or for the short deletion

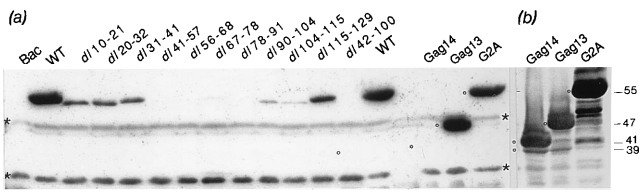

FIG. 3. (a) NW blot analysis of Pr55^{gag} and N-myristylated MA *dl* mutants. Lanes: Bac, BacPak6-infected cell extract; WT, Gag12myr+; G2A, unmyristylated full-length Gag; Gag13myr+, p6-p1-deleted Gag; Gag14myr+, p15-deleted Gag. Asterisks indicate background bands. (b) Western blot (immunoblot) corresponding to the right portion of the NW blot, showing the control lanes of Gag14, Gag13, and G2A, after immunoreaction with MAb anti-Pr55-p24. The positions of full-length Pr55^{gag}, Pr47^{gag} (p6-p1 deleted), Pr41^{gag} (p15 deleted), and Pr39^{gag} (p17 deleted), visible on the Western blot, are indicated by open dots.

mutants *dl*41-57myr+, *dl*56-68myr+, and *dl*78-91myr+. The binding was drastically reduced for *dl*67-78myr+, which bound to the probe at 1 to 2% of the WT level, and for *dl*90-104myr+ and *dl*104-115myr+ (3 to 5% of the WT level). The other *dl* mutants bound to the probe at levels significantly lower than the WT level, i.e., 15 to 20% of the WT level for *dl*10-21myr+, *dl*20-32myr+, and *dl*31-41myr+ and 30 to 35% of the WT level for *dl*115-129myr+. The absence of an RNA signal associated with mutants *dl*41-57myr+ and *dl*42-100myr+ was expected, since they accumulated Pr39^{gag}, a Gag precursor product which fails to bind to psi-RNA probe in NW blotting despite its intact NC domain, as shown with *in*40 (7). In the unmyristylated series, no deletion mutant, except *dl*115-129myr−, was found to have any detectable affinity for the riboprobe under the standard conditions used (not shown). This result and the absence of RNA binding shown by *dl*56-68myr+ and *dl*78-91myr+ strongly suggested that a key role is played by the N-myristylated MA domain, and more specifically its central region, in the overall conformation of the full-length Gag precursor and the subsequent affinity of its NC domain for viral RNA (7).

Extracellular release of particulate and soluble Gag precursor by MA *dl* mutants. The effect in *cis* of the MA deletions on the efficiency of Gag particle budding and release in the culture fluid of cells infected by the N-myristylated form of each *dl* mutant was immunologically assayed at 48 h p.i. The level of soluble Gag secretion in the culture fluid of cells expressing the unmyristylated versions of the *dl* mutants was also assayed. As shown in Fig. 4, Gag budding was almost totally abolished for mutants *dl*41-57myr+, *dl*56-68myr+, *dl*67-78myr+, and *dl*42-100myr+. The *dl*41-57myr+ phenotype could be due to an indirect phenomenon, i.e., it could result from the instability and intracellular proteolytic cleavage of *dl*41-57myr+ Gag precursor at the p17-p24 junction (Fig. 2a), which generated a p17-lacking, budding-defective Pr39^{gag} product. The other mutant patterns suggested the existence of a region in the MA, within amino acids 56 to 78, which was critical for assembly, budding, and extracellular release of N-myristylated Gag particles from the plasma membrane.

This region overlapped but did not completely coincide with

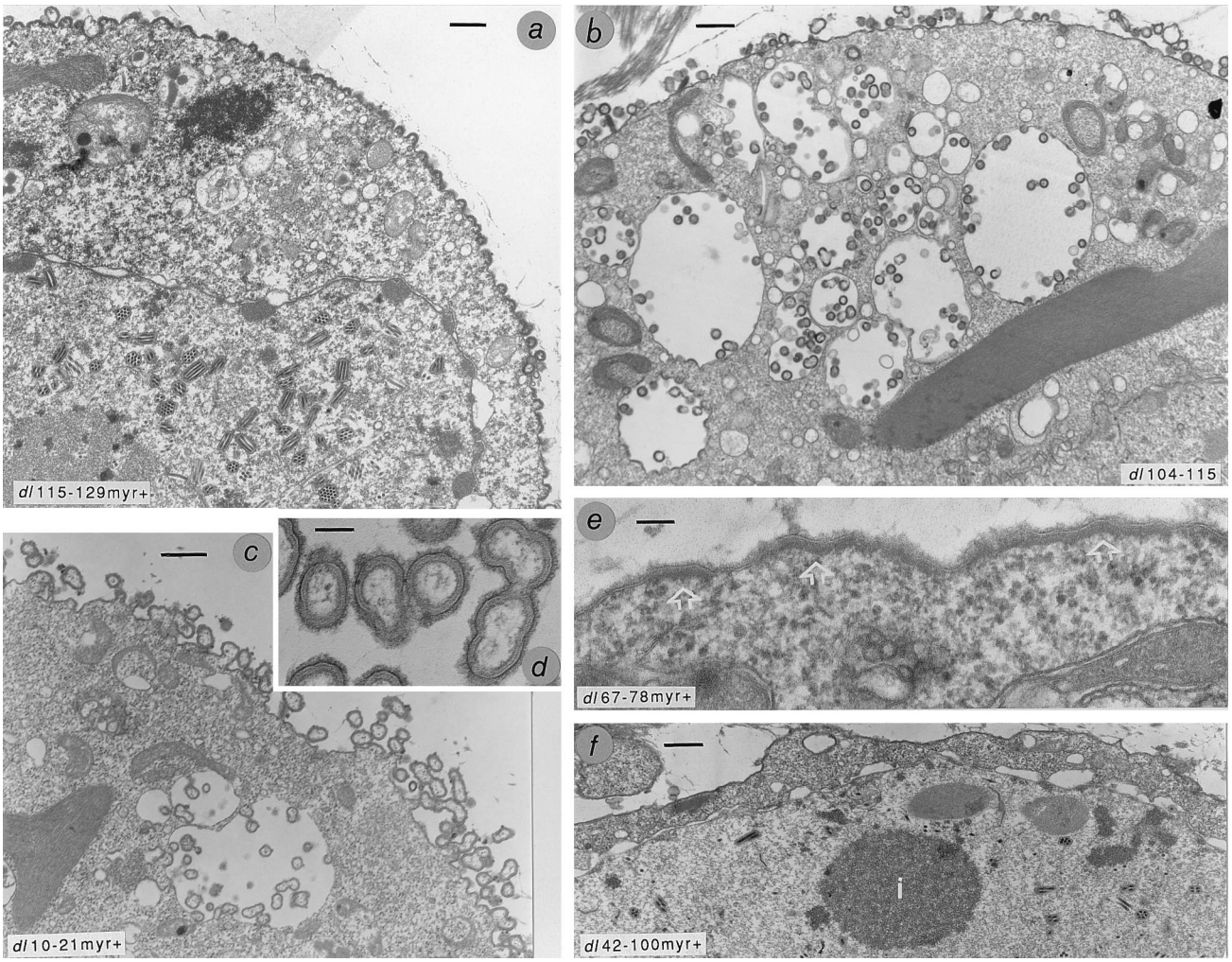

FIG. 5. EM analysis of Sf9 cells expressing N-myristylated *dl* mutants belonging to different phenotypic groups. Cells expressing group I (a), group II (b), group III (c and d), and group IV (e and f) mutants are shown. Cells were harvested at 48 h p.i. White arrows in panel e point to dense material accumulated at the inner leaflet of the plasma membrane; (f) i, nuclear inclusion. Bars, 500 nm (a, b, c, and f) and 100 nm (d and e).

the one required for the secretion of unmyristylated, soluble Gag precursor. The level of extracellular Gag was found to be drastically reduced for *dl*41-57myr− and *dl*56-68myr−, as well as for the large deletion mutant *dl*42-100myr− (Fig. 4). Since the Gag precursor of *dl*41-57myr− was not spontaneously cleaved into $Pr39^{gag}$, in contrast to its N-myristylated version, *dl*41-57myr+, the secretion-defective phenotype of the *dl*41-57myr− mutant was not due to the indirect mechanism of p17 removal. It rather implied that a direct role was played by the 41-57 deletion in the Gag secretion process. Taken altogether, these results identified a region in the MA, spanning residues 41 to 68, of which deletion was deleterious to soluble Gag release.

***cis* effects of MA deletions on Gag particle assembly.** The assembly phenotypes of the *dl* mutants were examined with the electron microscope. No intracellular particles were found with the unmyristylated *dl* mutants, and only amorphous inclusions of recombinant material were occasionally seen (data not shown). Likewise, no visible assemblies were found with any of the three recombinant MA proteins expressed by *amb*120, *amb*143, or *och*180, in contrast to the particulate structures observed with simian immunodeficiency virus MA expressed in recombinant vaccinia virus-infected cells (16). On the other hand, the phenotypes of the N-myristylated *dl* mutants could be arranged into four morphogenetic groups. The group I phenotype consisted of the WT budding pattern, and it was represented by a single mutant, *dl*115-129myr+ (Fig. 5a). Group II mutants exhibited a redistribution of Gag particles, with particles found rarely at the cell surface but in high numbers within intracytoplasmic, smooth-surfaced vesicles. This was the case for *dl*20-32myr+ and *dl*104-115myr+ and to a lesser extent for *dl*31-41myr+ (Fig. 5b). Group III mutants, *dl*10-21myr+, *dl*78-91myr+, and *dl*90-104myr+, showed extracellular and budding Gag particles that were very heterogeneous and irregular in shape and size (Fig. 5c and d). Group IV consisted of budding-defective mutants showing dense material at the inner leaflet of the plasma membrane and occasionally intranuclear amorphous inclusions (Fig. 5e and f). This group contained *dl*41-57myr+, *dl*56-68myr+, *dl*67-78myr+, and *dl*42-100myr+, which had the same assembly phenotype as the CA substitution mutant L268P (20). Thus, EM analysis confirmed that the integrity of the central region of the MA (residues 41 to 78) was essential for assembly,

budding, and extracellular release of N-myristylated Gag particles.

Complementation assays and *trans* dominance. A positive complementation effect between two MA deletion mutants would suggest the existence of separate functional subdomains in the MA which compensate for each other upon coexpression. Possible mutual rescue between *dl* mutants for Gag particle assembly and budding was thus investigated by pairwise coinfections of Sf9 cells and assays of extracellular Gag in the culture fluid. With the exception of pairs involving *dl*115-129myr+, which showed some complementation effect with other deletions located at the MA N-terminal extremity, there was no significant degree of rescue in *trans* between the MA *dl* mutants (data not shown). On the contrary, some *trans*-dominant negative effect was observed with most of the mutant pairs involving *dl*41-57myr+, *dl*56-68myr+, *dl*67-78myr+, and *dl*78-91myr+ (data not shown). The *trans*-dominant negative effect of MA deletion mutants on Gag particle assembly and budding over the WT Pr55^{gag} was analyzed by coinfections of each N-myristylated and unmyristylated *dl* mutant with WT Pr55^{gag}-expressing Gag12myr+. Extracellular release of Gag particles was significantly decreased in coinfections of Gag12myr+ with mutants *dl*41-57myr+, *dl*56-68myr+, *dl*67-78myr+, and *dl*78-91myr+ (to 25 to 30% of the control level), but not as great a detectable effect was observed with their unmyristylated counterparts (data not shown). A significant negative effect was obtained in coinfections of Gag12myr+ with two mutants expressing recombinant MA proteins, *amb*120 and *och*180, in which release was decreased to 10 and 20% of the control level, respectively. Similar effects were observed when their N-myristylated or unmyristylated versions were used (data not shown).

EM analysis of coinfected cells. The mechanisms of the *trans*-dominant negative effect exerted by some of our deletion and truncated Gag mutants on Gag particle assembly and release were examined at the cellular level with the electron microscope. Three types of EM patterns were observed in coexpression of Gag12myr+ with the N-myristylated MA *dl* mutants. (i) In the first pattern, there was no discernible change in the morphology and size of the budding Gag particles, compared with the morphology and size observed for single infection with Gag12myr+. This was the case for *dl*10-21, *dl*20-32, *dl*31-41, *dl*78-91, *dl*90-104, *dl*104-115, and *dl*115-129 (data not shown; Fig. 5a). (ii) The second pattern, shown by *dl*41-57, *dl*56-68, and *dl*67-78, consisted of irregular budding Gag particles, and it was similar to the pattern presented in Fig. 5 (panels c and d). (iii) In the third case, examplified by the coexpression of WT Pr55^{gag} and the *dl*42-100 mutant, cells exhibited rare budding Gag particles and intranuclear inclusions of recombinant proteins (data not shown; refer to Fig. 5f).

In cells coexpressing WT Pr55^{gag} and Gag truncated mutants, three morphological aspects could be distinguished. With *amb*143 in its N-myristylated or unmyristylated version, no significant change from the WT Gag particle budding pattern was observed (Fig. 6a and b). By contrast, drastic modifications in the cellular distribution of Gag particles were observed with the two other MA-expressing recombinants, *amb*120myr+ (or *amb*120myr−) and *och*180myr+ (or *och*180 myr−). Rare extracellular Gag particles were visible at the surfaces of cells coinfected with Gag12myr+ and *amb*120, and Gag particles accumulated within intracytoplasmic vesicles (Fig. 6c). In coexpression of WT Pr55^{gag} and *och*180, Gag particles were very rarely detected at the cell surface. Most of the core-like particles were found to accumulate intracellularly, sometimes in the cytoplasm (see Fig. 7f) but mainly within densely staining patches associated with the nucleus. The same effect was observed with both versions, *och*180myr+ and *och*180myr− (Fig. 6d and e).

EM-ARG of [^{3}H]myristyl-labeled recombinant-infected cells. The nuclear localization pattern of Gag particles in cells coinfected with Gag12myr+ (expressing WT Pr55^{gag}) and mutant *och*180 was reminiscent of the one shown by cells infected solely with N-myristylation-defective full-length recombinant Gag10 or G2A (7, 35). It could therefore be hypothesized that this topological effect resulted from the depletion of cellular pools of myristic acid due to a higher efficiency of N myristylation of the recombinant Gag protein expressed by the *och*180 mutant. However, the observation that the *och*180myr− mutant, which had lost its N-myristyl acceptor site by G2A substitution (7), induced the same nuclear retargeting of Gag particles as *och*180myr+ did argue against this hypothesis. Nevertheless, the possibility that *och*180myr+ and *och*180 myr− competed with N-myristyl transferase systems, via other residues of their N-terminal sequences (22), could not be excluded.

To address this issue, cells singly infected or coinfected with Gag12myr+ and each of the three truncated Gag mutants *amb*120, *amb*143, and *och*180 in their N-myristylated or unmyristylated versions were labeled with [^{3}H]myristic acid. Cell extracts were analyzed by SDS-PAGE and fluorography, and cell sections were examined by EM-ARG. In the case of uninfected Sf9 cells, no cellular protein was substantially labeled with [^{3}H]myristic acid under our conditions, and minute amounts of labeling were found in two discrete bands migrating at 8 and 20 kDa (Fig. 7e, lane 2). In the case of parental baculovirus (BacPAK6)-infected cells, however, two prominent labeled proteins, migrating as a major species at 16 kDa and a minor species at 28 kDa (Fig. 7e, lane 3), were visible. An extra band of [^{3}H]myristyl-labeled recombinant Pr55^{gag} was seen in the Gag12myr+-infected cell pattern (Fig. 7e, lane 4). In control cells infected with parental BacPAK6 or recombinant *och*180myr− and examined by EM-ARG, the [^{3}H]myristyl labeling was mainly localized in the vicinity of intranuclear baculovirions (Fig. 7d). In cells solely expressing WT Pr55^{gag}, numerous grains of ^{3}H label were found near the cell surface, associated with budding particles (Fig. 7a). Occasionally, silver grains were seen in rows ending at the plasma membrane (Fig. 7b). This feature was reminiscent of the arrangement of electron-dense spheres of 20 to 25 nm in diameter observed by conventional EM (Fig. 7c), and it was suggestive of a cytoplasmic transit of [^{3}H]myristyl-labeled Pr55^{gag} oligomers (9a) leading to budding particles. No significant difference in the EM-ARG patterns of cells singly infected with Gag12myr+, cells coinfected with Gag12myr+ and *amb*143, and cells coinfected with Gag12myr+ and *amb*120 was found (data not shown). However, in cells coinfected with Gag12myr+ and the mutant *och*180myr−, the nucleoplasm, and occasionally the cytoplasm, showed Gag core-like particles associated with [^{3}H]myristyl-label (Fig. 7f and g). This suggested that at least some of the WT Pr55^{gag} molecules which were retargeted to the nucleus upon *och*180myr− coexpression were N myristylated.

DISCUSSION

A panel of mutants with deletions in the MA domain of the HIV-1 Gag precursor were constructed and expressed in insect cells infected by recombinant baculoviruses. The three-dimensional modifications induced by the mutations were indirectly analyzed by the susceptibility of Pr55^{gag} to HIV-1 protease coexpressed in *trans* in coinfected cells (7, 20) and its affinity in

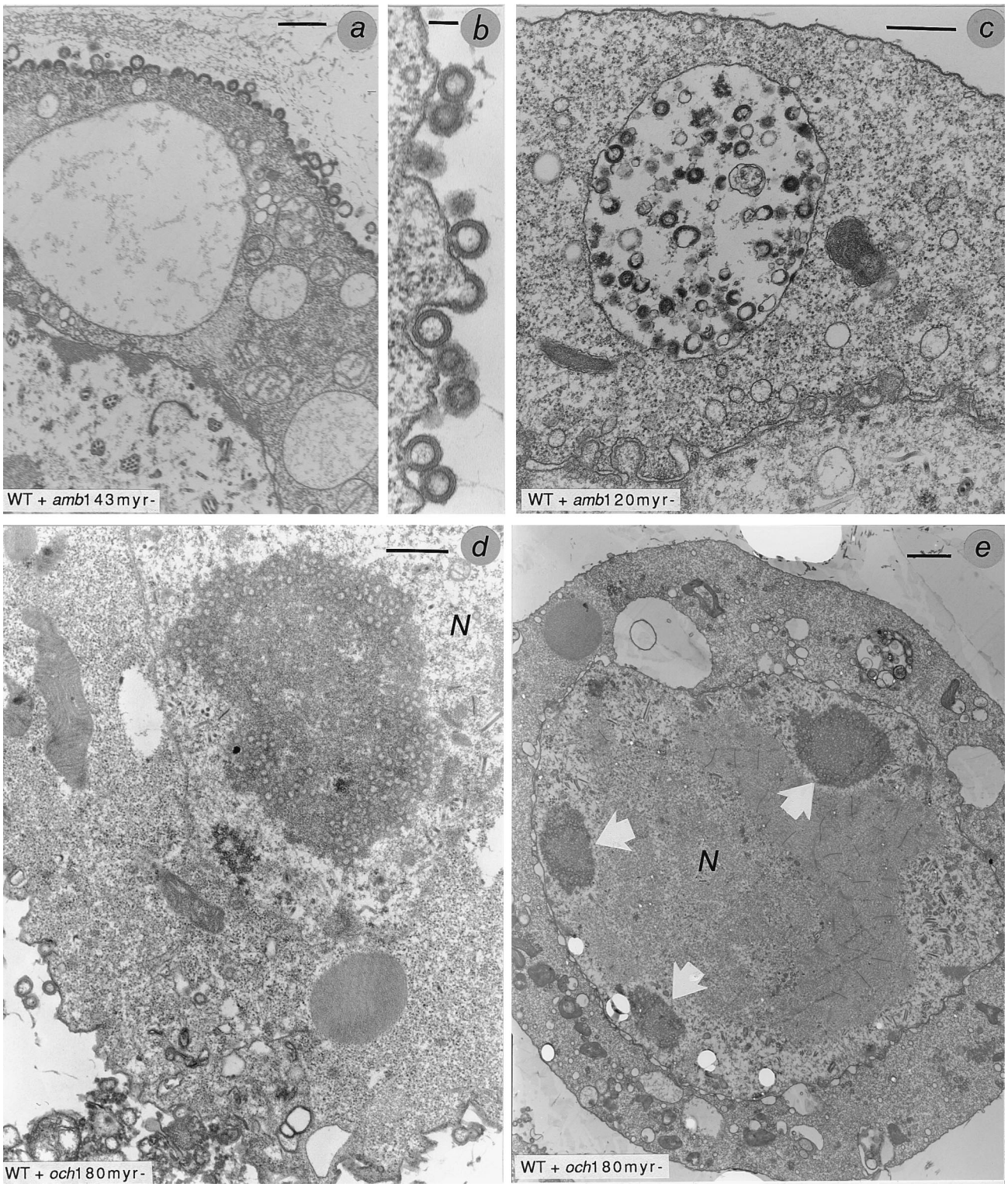

FIG. 6. EM analysis of doubly infected Sf9 cells coexpressing WT $Pr55^{gag}$ and unmyristylated truncated Gag mutants in *trans*. (a and b) *amb*143myr−. (c) *amb*120myr−. (d and e) *och*180myr−. White arrows in panel e point to Gag particles assembled within the nucleus, and these particles are shown in panel d at a higher magnification. Note the presence of rare budding particles at the cell surface shown in panel d. Bars, 500 nm (a, c, and d), 100 nm (b), and 1 μm (e).

vitro for a viral probe containing the encapsidation signal (7, 21, 24). The capacities of the Gag mutants to self-assemble and to be released as membrane-enveloped particles by budding from the plasma membrane or to be secreted as soluble, unassembled Gag polyproteins were analyzed. The culture media of cells infected with recombinants expressing N-myristylated or unmyristylated versions of the same mutants, respectively, were immunologically assayed. The assembly pheno-

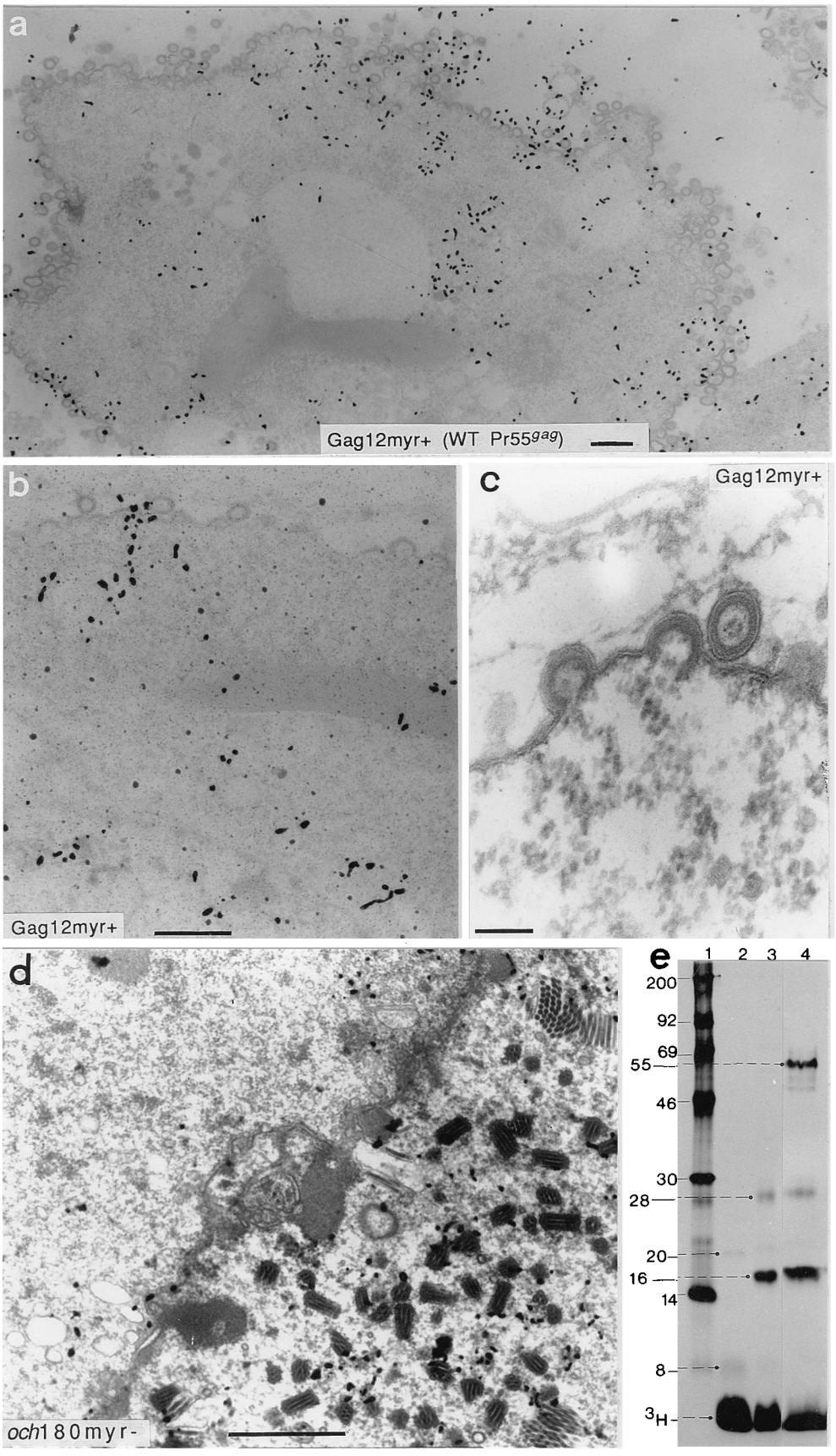
a
Gag12myr+ (WT Pr55gag)
b
Gag12myr+
c
Gag12myr+
d
och180myr-
e
1 2 3 4
200
92
69
55
46
30
28
20
16
14
8
3H

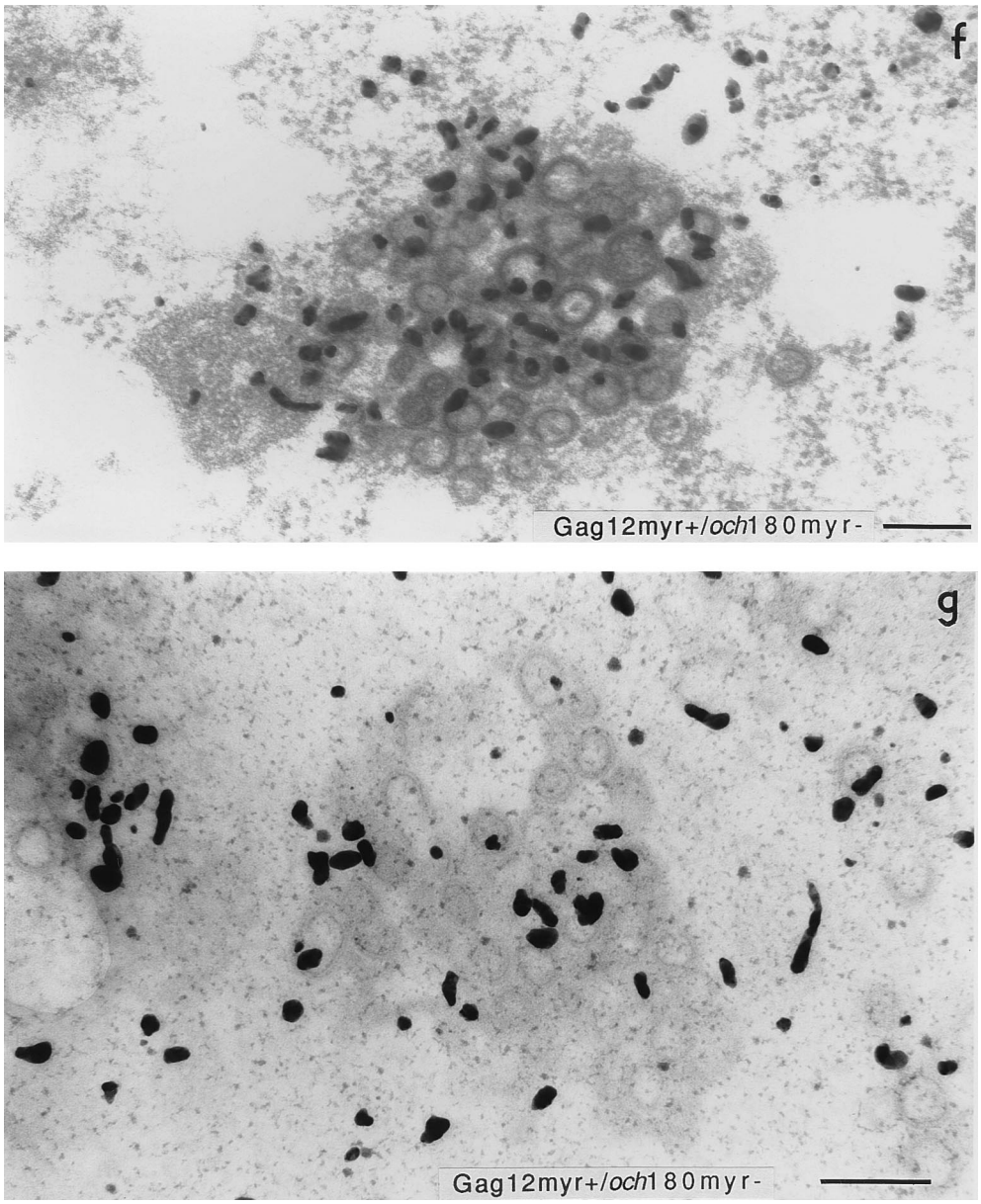

FIG. 7. Autoradiographic analysis of recombinant-infected Sf9 cells labeled with [^{3}H]myristic acid (4-week exposure). (a through c) Cells singly infected with Gag12myr+ and analyzed by EM-ARG (a and b) or conventional EM (c). (d) EM-ARG of single infection with Gag carboxy-truncated mutant *och*180myr−. (e) SDS-PAGE and fluorography of ^{14}C-labeled protein markers (lane 1), extracts from mock-infected cells (lane 2), and cells infected with parental baculovirus (lane 3) or recombinant Gag12myr+ (lane 4). Numbers at the left are molecular masses in kilodaltons. ^{3}H, soluble [^{3}H]myristic acid. (f and g) EM-ARG of cells coexpressing WT Pr55^{gag} (Gag12myr+) and mutant *och*180myr−, showing Gag particles within the cytoplasm (f) and the nucleoplasm (g). Bars, 500 nm (a and b), 100 nm (c), 1 μm (d), and 200 nm (f and g).

types and cellular compartmentalization of the N-myristylated Gag mutants were also analyzed by EM and EM-ARG.

One deletion in the MA domain, located between residues Gly-56 and Leu-68, was found to have common deleterious effects on all the biological properties of Gag precursor assayed here, i.e., (i) assembly and budding of N-myristylated Gag particles, (ii) extracellular release of unmyristylated soluble Gag polyproteins, (iii) in vivo processing by HIV-1 protease coexpressed in *trans*, and (iv) affinity for a psi-containing viral RNA probe in NW blotting. In addition, a discrete *trans*-dominant negative effect on Gag particle assembly and budding was observed in coexpression of WT Pr55^{gag} and the *dl*56-68 mutant. The region deleted from this mutant, G-CRQILGQLQPS-L, corresponds to a cysteine-containing, L(I)-Q-rich sequence, which has been found to adopt an alpha helix conformation (1, 24a). The MA central domain within residues 41 to 78 has already been determined to be essential for virus assembly and incorporation of envelope glycoproteins into the virions (9, 44, 48). Moreover, a cluster of single-amino-acid substitutions within residues 55 to 59 (12), or the use of a competing synthetic peptide mimicking the MA sequence from residues 47 to 59 (27), abolished virus particle assembly and infectious virus production.

The deletion of the C-terminal portion of the MA, and more specifically of the conserved sequence 119-AADTGHSNQV-128, has been shown to be detrimental to the early steps of the

viral life cycle, most likely at the stage of virus entry (49). However, our mutant *dl*115-129myr+, which lacked this sequence, presented a WT assembly phenotype, suggesting that this MA region was not essential for the self-assembly process of Gag precursor molecules in insect cells. This was confirmed by other point mutations in this portion of the MA (9, 12). In particular, substitutions at residues 119, 120, 127, and 129 did not significantly affect virus particle assembly in transfected HeLa cells or the release of the particles from these cells (12).

Three MA mutants, with total (*dl*20-32myr+ and *dl*104-115myr+) or partial (*dl*31-41myr+) deletion of one or the other of the two polybasic signals, failed to transport N-myristylated Gag precursor to the plasma membrane and instead accumulated Gag particles within intracytoplasmic vesicles (Fig. 5c). Our results with insect cells were consistent with the observation that deletion or substitutions in the polybasic region of the MA domain between residues 26 and 32 greatly affected the intracellular transport of the Gag precursor in transfected COS-7 cells (50). This would suggest that the MA polybasic signals have key roles in cellular transport, targeting, and binding to the plasma membrane, confirming previous results (10, 39, 50, 51). However, substitutions of Lys residues at MA positions 26, 27, and 32 resulted in only a slight delay in peak virus production by CEM cells and a twofold reduction in particle assembly in and release from transfected HeLa cells (12). This apparent discrepancy between different reports favors the hypothesis that some MA sequences will act as transport signals only in certain cell or virus systems (12).

Coinfection of Gag12myr+ with *amb*143myr+ or *amb*143 myr− resulted in a normal budding pattern for WT Gag particles at the plasma membrane (Fig. 6a and b). By contrast, a significant *trans*-dominant negative effect (40) on WT Gag particle assembly and budding was observed in coexpression of WT Pr55^{gag} with *amb*120 or *och*180. This negative effect was apparently due to a massive retargeting of Gag particles to cytoplasmic vesicles in the case of *amb*120 and to the nucleus in the case of *och*180 (Fig. 6c through e). The same topological effect was obtained regardless of the mutant's N-terminal modification, i.e., with N-myristylation-competent *amb*120 myr+ or N-myristylation-defective *amb*120myr− on the one hand, and with *och*180myr+ or *och*180myr− on the other hand. This suggested that the Gag particle relocalization did not result from a competition for cellular N-myristyl transferases between WT Pr55^{gag} and coexpressed recombinant MA protein. Moreover, EM-ARG of [^{3}H]myristyl-labeled cells coexpressing WT Pr55^{gag} and *och*180myr− showed that Gag precursor molecules assembled into core-like particles within the cytoplasm (Fig. 7f) and the nucleus (Fig. 7g) were indeed N myristylated.

The different patterns of Gag particle relocation occurring upon *amb*120 and *och*180 coexpression in *trans*, and the resulting *trans*-dominant negative effect on budding and extracellular release of WT Gag particles, suggested that the recombinant Gag proteins of *amb*120 and *och*180 competed with at least two separate topogenic signals in WT Pr55^{gag}. (i) One would be involved in myristyl-dependent plasma membrane targeting of Gag and would be localized in the first 120 amino acids of the MA. (ii) The other one would be involved in the cytoplasmic anchorage of Gag and would be situated between residues 143 and 180 in the CA domain. This hypothesis is consistent with the model of a dominant bipartite membrane-targeting and binding signal determined to be present in the amino-terminal 31 amino acids of HIV-1 Pr55^{gag} (51). It is also supported by recent results suggesting the existence of an MA region downstream of the myristylation site which is required for transport of Gag precursor to the plasma membrane and for stable membrane binding (39). The relevance of the intranuclear localization of N-myristylated Pr55^{gag} molecules to the life cycle of the virus, as well as the identities of the cellular partners participating in their nuclear transport and cytoplasmic anchorage processes, remains to be elucidated.

ACKNOWLEDGMENTS

This work was supported by the Agence Nationale de Recherche sur le SIDA, the Centre National de la Recherche Scientifique, the Fondation pour la Recherche Médicale, the Fédération des Groupements d'Entreprises Françaises dans la Lutte contre le Cancer, and the Association Les Bons Copains de Tain-l'Hermitage.

We are grateful to XiaoFang Yu for providing the plasmids harboring the D1 to D10 deletions, to Saw See Hong for critical reading of the manuscript, and to Liliane Cournud for secretarial aid.

REFERENCES

1. **Andreassen, H., H. Bohr, J. Bohr, S. Brunak, T. Bugge, R. M. J. Cotterill, C. Jacobsen, P. Kusk, B. Lautrup, S. B. Petersen, T. Særmark, and K. Ulrich.** 1990. Analysis of the secondary structure of the human immunodeficiency virus (HIV) proteins p17, gp120, and gp41 by computer modeling based on neural network methods. J. Acquired Immune Defic. Syndr. **3:**615–622.
2. **Blomberg, J., and P. Medstrand.** 1990. A sequence in the carboxylic terminus of the HIV-1 matrix protein is highly similar to sequences in membrane-associated proteins of other RNA viruses: possible functional implications. New Biol. **2:**1044–1046.
3. **Bouteille, M.** 1976. The "LIGOP" method for routine ultrastructural autoradiography. A combination of single grid coating, gold latensification and Phenidon development. J. Microsc. Biol. Cell. **27:**121–127.
4. **Bryant, M., and L. Ratner.** 1990. Myristoylation-dependent replication and assembly of human immunodeficiency virus 1. Proc. Natl. Acad. Sci. USA **87:** 523–527.
5. **Bukrinskaya, A. G., G. K. Vorkunova, and Y. Y. Tentsov.** 1992. HIV-1 matrix protein p17 resides in cell nuclei in association with genomic RNA. AIDS Res. Hum. Retroviruses **8:**1795–1801.
6. **Bukrinsky, M., S. Haggerty, M. P. Dempsey, N. Sharova, A. Adzhubel, L. Spitz, P. Lewis, D. Goldfarb, M. Emerman, and M. Stevenson.** 1993. A nuclear localization signal within HIV-1 matrix protein that governs infection of non-dividing cells. Nature (London) **365:**666–669.

6a. **Carrière, C., B. Gay, N. Chazal, N. Morin, and P. Boulanger.** Sequence requirements for encapsidation of deletion mutants and chimeras of human immunodeficiency virus type 1 Gag precursor into retrovirus-like particles. Submitted for publication.

7. **Chazal, N., C. Carrière, B. Gay, and P. Boulanger.** 1994. Phenotypic characterization of insertion mutants of the human immunodeficiency virus type 1 Gag precursor expressed in recombinant baculovirus-infected cells. J. Virol. **68:**111–122.
8. **Crawford, S., and S. P. Goff.** 1984. Mutations in *gag* proteins p12 and p15 of Moloney murine leukemia virus block early stages of infection. J. Virol. **49:** 909–917.
9. **Dorfman, T., F. Mammano, W. A. Haseltine, and H. G. Göttlinger.** 1994. Role of the matrix protein in the virion association of the human immunodeficiency virus type 1 envelope glycoprotein. J. Virol. **68:**1689–1696.

9a. **Ehrlich, L. S., B. E. Agresta, and C. A. Carter.** 1992. Assembly of recombinant human immunodeficiency virus type 1 capsid protein in vitro. J. Virol. **66:**4874–4883.

10. **Fäcke, M., A. Janetzko, R. L. Shoeman, and H.-G. Kräusslich.** 1993. A large deletion in the matrix domain of the human immunodeficiency virus *gag* gene redirects virus particle assembly from the plasma membrane to the endoplasmic reticulum. J. Virol. **67:**4972–4980.
11. **Fakan, S., and J. Fakan.** 1987. Autoradiography of spread molecular complexes, p. 201–214. *In* J. Sommerville and U. Scheer (ed.), Electron microscopy in molecular biology, a practical approach. IRL Press, Oxford.
12. **Freed, E. O., J. M. Orenstein, A. J. Buckler-White, and M. A. Martin.** 1994. Single amino acid changes in the human immunodeficiency virus type 1 matrix protein block virus particle production. J. Virol. **68:**5311–5320.
13. **Gelderblom, H. R.** 1991. Assembly and morphology of HIV: potential effect of structure on viral function. AIDS **5:**617–638.
14. **Gelderblom, H. R., E. H. S. Hausmann, M. Ozel, G. Pauli, and M. A. Koch.** 1987. Fine structure of human immunodeficiency virus (HIV) and immunolocalization of structural proteins. Virology **156:**171–176.
15. **Gheysen, D., E. Jacobs, F. de Foresta, C. Thiriart, M. Francotte, D. Thines, and M. De Wilde.** 1989. Assembly and release of HIV-1 precursor Pr55^{gag} virus-like particles from recombinant baculovirus-infected insect cells. Cell **59:**103–112.

16. **Gonzalez, S. A., J. L. Affranchino, H. R. Gelderblom, and A. Burny.** 1993. Assembly of the matrix protein of simian immunodeficiency virus into virus-like particles. Virology **194:**548–556.
17. **Göttlinger, H. G., J. G. Sodroski, and W. A. Haseltine.** 1989. Role of capsid precursor processing and myristoylation in morphogenesis and infectivity of human immunodeficiency virus type 1. Proc. Natl. Acad. Sci. USA **86:**5781–5785.
18. **Guan, K. L., and J. E. Dixon.** 1991. Eukaryotic proteins expressed in *Escherichia coli*: an improved thrombin cleavage and purification procedure of fusion proteins with glutathione *S*-transferase. Anal. Biochem. **192:**262–267.
19. **Hendersson, L. E., M. A. Bowers, R. C. Sowder II, S. A. Serabyn, D. G. Johnson, J. W. Bess, Jr., L. O. Arthur, D. K. Bryant, and C. Fenselau.** 1992. Gag proteins of the highly replicative MN strain of human immunodeficiency virus type 1: posttranslational modifications, proteolytic processings, and complete amino acid sequences. J. Virol. **66:**1856–1865.
20. **Hong, S. S., and P. Boulanger.** 1993. Assembly-defective point mutants of the immunodeficiency virus type 1 Gag precursor phenotypically expressed in recombinant baculovirus-infected cells. J. Virol. **67:**2787–2798.
21. **Jowett, J. B. M., D. J. Hockley, M. V. Nermut, and I. M. Jones.** 1992. Distinct signals in HIV-1 Pr55 necessary for RNA binding and particle formation. J. Gen. Virol. **73:**3079–3086.
22. **Kaplan, J. M., G. Mardon, J. M. Bishop, and H. E. Varmus.** 1988. The first seven amino acids encoded by the v-*src* oncogene act as a myristylation signal: lysine 7 is a critical determinant. Mol. Cell. Biol. **8:**2435–2441.
23. **Laemmli, U. K.** 1970. Cleavage of structural proteins during the assembly of the head of bacteriophage T4. Nature (London) **227:**680–685.
24. **Luban, J., and S. P. Goff.** 1991. Binding of human immunodeficiency virus type 1 (HIV-1) RNA to recombinant HIV-1 *gag* polyprotein. J. Virol. **65:**3203–3212.
24a. **Matthews, S., P. Barlow, J. Boyd, G. Barton, R. Russell, H. Mills, M. Cunningham, M. Meyers, N. Burns, N. Clark, S. Kingsman, A. Kingsman, and I. Campbell.** 1994. Structural similarity between the p17 matrix protein of HIV-1 and interferon-γ. Nature (London) **370:**666–668.
25. **Mervis, R. J., N. Ahmad, E. P. Lillehoj, M. G. Raum, F. H. R. Salazar, H. W. Chan, and S. Venkatesan.** 1988. The *gag* gene products of human immunodeficiency virus type 1: alignment within the *gag* open reading frame, identification of posttranslational modifications, and evidence for alternative Gag precursors. J. Virol. **62:**3993–4002.
26. **Nermut, M. V., D. J. Hockley, J. B. M. Jowett, I. A. Jones, M. Garreau, and D. Thomas.** 1994. Fullerene-like organization of HIV gag-protein shell in virus-like particles produced by recombinant baculovirus. Virology **198:**288–296.
27. **Niedrig, M., H. S. Gelderblom, G. Pauli, J. März, H. Bickhardt, H. Wolf, and S. Modrow.** 1994. Inhibition of infectious human immunodeficiency virus type 1 particle formation by Gag protein-derived peptides. J. Gen. Virol. **75:**1469–1474.
27a. **Niedrig, M., J. Hinkula, W. Weigelt, J. L'Age-Stehr, G. Pauli, J. Rosen, and B. Wahren.** 1989. Epitope mapping of monoclonal antibodies against human immunodeficiency virus type 1 structural proteins by using peptides. J. Virol. **63:**3525–3528.
28. **Pal, R., M. S. Reitz, Jr., E. Tschachler, R. C. Gallo, M. G. Sarngadharan, and F. D. M. Veronese.** 1990. Myristoylation of *gag* polyproteins of HIV-1 plays an important role in virus assembly. AIDS Res. Hum. Retroviruses **6:**721–730.
29. **Park, J., and C. D. Morrow.** 1992. The nonmyristylated $Pr160^{gag\text{-}pol}$ polyprotein of human immunodeficiency virus type 1 interacts with $Pr55^{gag}$ and is incorporated into viruslike particles. J. Virol. **66:**6304–6313.
30. **Rein, A., M. R. McClure, N. R. Rice, R. B. Luftig, and A. M. Schultz.** 1986. Myristylation site in $PR65^{gag}$ is essential for virus particle formation by Moloney murine leukemia virus. Proc. Natl. Acad. Sci. USA **83:**7246–7250.
31. **Rhee, S. S., and E. Hunter.** 1987. Myristylation is required for intracellular transport but not for assembly of of D-type retrovirus capsids. J. Virol. **61:**1045–1053.
32. **Rhee, S. S., and E. Hunter.** 1990. A single amino acid substitution within the matrix protein of a type D retrovirus converts its morphogenesis to that of a type C retrovirus. Cell **63:**77–86.
33. **Rhee, S. S., and E. Hunter.** 1990. Structural role of the matrix protein of type D retroviruses in Gag polyprotein stability and capsid assembly. J. Virol. **64:**4383–4389.
34. **Rhee, S. S., and E. Hunter.** 1991. Amino acid substitutions within the matrix protein of type D retroviruses affect assembly, transport and membrane association of a capsid. EMBO J. **10:**535–546.
35. **Royer, M., M. Cerutti, B. Gay, S. S. Hong, G. Devauchelle, and P. Boulanger.** 1991. Functional domains of HIV-1 *gag*-polyprotein expressed in baculovirus-infected cells. Virology **184:**417–422.
36. **Royer, M., S.-S. Hong, B. Gay, M. Cerutti, and P. Boulanger.** 1992. Expression and extracellular release of human immunodeficiency virus type 1 Gag precursors by recombinant baculovirus-infected cells. J. Virol. **66:**3230–3235.
37. **Sanger, F., S. Nicklen, and A. R. Coulson.** 1977. DNA sequencing with chain-terminating inhibitors. Proc. Natl. Acad. Sci. USA **74:**5463–5467.
38. **Schultz, A. M., and A. Rein.** 1989. Unmyristylated Moloney murine leukemia virus $Pr55^{gag}$ is excluded from virus assembly and maturation events. J. Virol. **63:**2370–2373.
39. **Spearman, P., J.-J. Wang, N. Vander Heyden, and L. Ratner.** 1994. Identification of human immunodeficiency virus type 1 Gag protein domains essential to membrane binding and particle assembly. J. Virol. **68:**3233–3242.
40. **Trono, D., M. B. Feinberg, and D. Baltimore.** 1989. HIV-1 Gag mutants can dominantly interfere with the replication of the wild-type virus. Cell **59:**113–120.
41. **Valverde, V., P. Lemay, J. M. Masson, B. Gay, and P. Boulanger.** 1992. Autoprocessing of the human immunodeficiency virus type 1 protease precursor expressed in *Escherichia coli* from a synthetic gene. J. Gen. Virol. **73:**639–651.
42. **Veronese, F. D. M., R. Rahman, T. D. Copeland, S. Oroszlan, R. C. Gallo, and M. G. Sarngadharan.** 1987. Immunological and chemical analysis of p6, the carboxyl-terminal fragment of HIV p15. AIDS Res. Hum. Retroviruses **3:**253–264.
43. **Wain-Hobson, S., P. Sonigo, O. Danos, S. Cole, and M. Alizon.** 1985. Nucleotide sequence of the AIDS virus, LAV. Cell **40:**9–17.
44. **Wang, C.-T., and E. Barklis.** 1993. Assembly, processing, and infectivity of human immunodeficiency virus type 1 Gag mutants. J. Virol. **67:**4264–4273.
45. **Wang, C.-T., Y. Zhang, J. McDermott, and E. Barklis.** 1993. Conditional infectivity of a human immunodeficiency virus matrix domain deletion mutant. J. Virol. **67:**7067–7076.
46. **Wills, J. W., and R. C. Craven.** 1991. Form, function, and use of retroviral gag proteins. AIDS **5:**639–654.
47. **Wills, J. W., R. C. Craven, R. A. Weldon, T. D. Nelle, and C. R. Erdie.** 1991. Suppression of retroviral MA deletions by the amino-terminal membrane-binding domain of $p60^{src}$. J. Virol. **65:**3804–3812.
48. **Yu, X., Q.-C. Yu, T.-H. Lee, and M. Essex.** 1992. The C terminus of human immunodeficiency virus type 1 matrix protein is involved in early steps of the virus life cycle. J. Virol. **66:**5667–5670.
49. **Yu, X., X. Yuan, Z. Matsuda, T.-H. Lee, and M. Essex.** 1992. The matrix protein of human immunodeficiency virus type 1 is required for incorporation of viral envelope protein into mature virions. J. Virol. **66:**4966–4971.
50. **Yuan, X., X. F. Yu, T. H. Lee, and M. Essex.** 1993. Mutations in the N-terminal region of human immunodeficiency virus type 1 matrix protein block intracellular transport of the Gag precursor. J. Virol. **67:**6387–6394.
51. **Zhou, W., L. J. Parent, J. W. Wills, and M. D. Resh.** 1994. Identification of a membrane-binding domain within the amino-terminal region of human immunodeficiency virus type 1 Gag protein which interacts with acidic phospholipids. J. Virol. **68:**2556–2569.